Am J Transl Res 2020;12(9):5433-5448
www.ajtr.org /ISSN:1943-8141/AJTR0112143

Original Article

Deubiquitinase PSMD7 regulates cell fate and is associated with disease progression in breast cancer

Yuanjie Zhao[1*], Xiaomei Yang[2*], Xinchun Xu[3], Jieru Zhang[4], Ling Zhang[5], Hui Xu[6], Zhiming Miao[1], Dawei Li[5], Shusheng Wang[1]

[1]Department of General Surgery, Affiliated Zhangjiagang Hospital of Soochow University, Suzhou 215600, Jiangsu, China; [2]Department of Emergency, Affiliated Zhangjiagang Hospital of Soochow University, Suzhou 215600, Jiangsu, China; [3]Department of Ultrasound, Affiliated Zhangjiagang Hospital of Soochow University, Suzhou 215600, Jiangsu, China; [4]Department of Respiratory and Critical Care Medicine, Affiliated Zhangjiagang Hospital of Soochow University, Suzhou 215600, Jiangsu, China; [5]Center for Translational Medicine, Affiliated Zhangjiagang Hospital of Soochow University, Suzhou 215600, Jiangsu, China; [6]Department of Thoracic Surgery, Affiliated Zhangjiagang Hospital of Soochow University, Suzhou 215600, Jiangsu, China. [*]Co-first authors.

Received April 8, 2020; Accepted August 22, 2020; Epub September 15, 2020; Published September 30, 2020

Abstract: Breast cancer is the most common malignant tumor and the leading cause of cancer-related death in women. The ubiquitin-proteasome system regulates the stability of most proteins controlling various biological processes in human cells. PSMD7, as a core component of the 26S proteasome, is critical for the degradation of ubiquitinated proteins in the proteasome. Currently, PSMD7 expression and its roles in the progression of breast cancer remain largely unknown. In this study, we assessed the level of PSMD7 in breast cancer tissues and investigated the underlying molecular events by which PSMD7 could play a role in tumor progression. The results showed that the PSMD7 level was significantly upregulated in breast cancer tissues. PSMD7 expression was closely associated with tumor subtype, tumor size, lymph node invasion, and TNM stage. A high PSMD7 level predicted poor overall survival (OS) and disease-free survival (DFS) in breast cancer patients. Furthermore, univariate Cox regression analysis indicated that lymph node invasion, distant metastasis, and PSMD7 expression were associated with OS and DFS. Multivariate regression analysis indicated that PSMD7 was an independent predictor of OS (HR=1.310, 95% CI=1.038-1.652). Importantly, PSMD7 knockdown induced cell cycle arrest in the G0/G1 phase, leading to cell senescence and apoptosis. PSMD7 knockdown inhibited the expression of key cell cycle-related proteins and promoted the stability of p21 and p27 in breast cancer cells. PSMD7 may be a valuable prognostic indicator and potential therapeutic target for breast cancer.

Keywords: Deubiquitinase, PSMD7, breast cancer, prognosis, cell cycle-related proteins

Introduction

Breast cancer is a complex malignant tumor derived from breast epithelial tissue. It is for the most common malignant cancer and the leading cause of cancer-related death in women. According to the Global Cancer Statistics of 2018, nearly every one in four cancer cases was breast cancer, and almost one in six cancer deaths was breast cancer related [1]. Four main subtypes of breast cancer are normally defined based on different hormone receptor levels: estrogen receptor (ER)-positive or progesterone receptor (PR)-positive and human epidermal growth factor receptor 2 (HER-2)-negative breast cancer is defined as luminal A; ER- or PR-positive and HER-2-positive breast cancer is defined as luminal B; HER-2-positive only breast cancer is defined as luminal HER-2; and breast cancer negative for all three receptors is defined as basal [2]. Currently, the main treatments for breast cancer are surgery, radiotherapy, cytotoxic drugs, and targeted therapy. With early screening, diagnosis, and intervention for breast cancer, the mortality and recurrence of breast cancer have been significantly reduced. However, many breast cancer patients do not benefit from adjuvant therapy due to the absence of well-defined molecular targets [3]. New molecular targets are urgently needed to

assess the progression and improve the treatment of the disease.

The ubiquitin-proteasome system plays an essential role in a variety of biological processes. More than 80% of cellular proteins are degraded through this important pathway, which is involved in regulating cellular function and maintaining homeostasis. The 26S proteasome is a multisubunit complex with a molecular weight of 2.5 MDa and is composed of two 19S regulatory particles and a 20S core particle [4]. Importantly, the 26S proteasome is critical for the degradation of substrates marked by polyubiquitin chains. Many studies have shown that the 26S proteasome is involved in cell cycle progression, apoptosis, transcription, DNA repair, protein quality control, and antigen presentation [5, 6]. Due to the critical role of the 26S proteasome in cell biological processes, especially in tumor cell growth and survival, inhibition of proteasome function has become a powerful strategy for anticancer therapy. Bortezomib, a proteasome inhibitor, has emerged as an effective drug target for clinical treatment. It can induce cell cycle arrest and apoptosis by disrupting various signaling pathways and NF-kB function in multiple myeloma [7].

Proteasome 26S subunit, non-ATPase 7 (PSMD7), also known as Rpn8 or Mov34, is an ATP-independent component of the 19S regulatory subunit and interacts with PSMD14 to form heterodimers as a functional complex that is extremely critical for ubiquitinated substrate degradation in the proteasome [8, 9]. Our recent study revealed that an upregulated PSMD14 level was associated with progressive disease status in lung adenocarcinoma via the regulation of p21 stability [10]. Although the role of PSMD14 as a component of the proteasome has been widely reported in many studies [11-13], the function of PSMD7 remains largely unknown. A previous study revealed that PSMD7 regulated the G2/M phase cell cycle transition during HIV infection [14]. The polymorphism rs17336700 in the PSMD7 gene is thought to be associated with ankylosing spondylitis [15]. PSMD7 knockdown induced cell apoptosis and inhibited tumorigenesis in esophageal squamous cell carcinoma [13]. However, PSMD7 expression in breast cancer tissues and its role in tumorigenesis remain to be determined. In this study, we explored the expression of PSMD7 and its potential role in modulating cell fate in breast cancer. We found that PSMD7 was significantly overexpressed in cancer tissues and that a high PSMD7 level was associated with poor clinical stages, OS, and DFS in breast cancer. The knockdown of PSMD7 can lead to cell cycle arrest, senescence, and apoptosis via regulation of key cell cycle proteins in breast cancer cells. These findings indicate that PSMD7 could be a prognostic indicator and promising therapeutic target in breast cancer.

Materials and methods

Patients

To determine PSMD7 expression in breast cancer, we purchased human breast invasive ductal carcinoma (IDC) tissue microarrays (#HBreD090CS01, Shanghai Outdo Biotech Company, Shanghai, China). The demographic and clinicopathological features of the patients in this study are shown in Table S1. We also used another cohort of 8 breast cancer patients enrolled at the Affiliated Zhangjiagang Hospital of Soochow University from September 2018 to November 2018. All of the patients underwent curative surgery for breast cancer without any previous adjuvant therapy. The diagnoses were confirmed by at least two experienced histological pathologists at the hospital. All of the oncology stages were determined according to the NCCN Breast Cancer Guidelines (http://www.NCCN.org). Breast cancer tissues were carefully isolated during surgery, and matched noncancerous breast tissues were collected at least one centimeter away from the edge of the lesion. The tissue samples were immediately stored at -80°C for further extraction of proteins and immunohistochemistry. The demographic, clinical, and pathological features of the patients are shown in Table S2. The research on human specimens was approved by Zhangjiagang Hospital's Institutional Review Board (No. 2019001). Written permission was requested and obtained from all of the patients in this study.

Bioinformatics analysis

We used publicly available clinical information from the cBioportal for Cancer Genomics (TCGA) database (http://www.cbioportal.org/) [16, 17], including basic demographic and clinical

information as well as survival status after surgery to assess the correlations between PSMD7, clinical pathological status, and patient survival in breast cancer. We retrieved clinical information from 1,082 breast cancer patients for correlation analysis. We selected the tumor patients in the upper and lower quartiles of PSMD7 expression and obtained 540 patients for OS analysis and 464 patients for DFS analysis. Patients with complete demographic and clinical information were also used for univariate and multivariate Cox regression analyses for OS and DFS, respectively.

Cell culture

The breast cancer cell lines MCF-7 and MDA-MB-231 were obtained from the American Type Culture Collection (ATCC, Manassas, VA, USA). The cells were cultured in Dulbecco's Modified Eagle Medium (DMEM) (Corning, Corning, NY, USA) supplemented with 10% FBS and antibiotics consisting of 100 U/ml penicillin and 100 μg/ml streptomycin in a humidified atmosphere at 37°C with 5% CO_2. The cells were passaged at 75-80% confluency every 2 to 3 days.

Western blotting and antibodies

Total proteins from the tissues and cells were isolated using FLAG lysis buffer (50 mM Tris·HCl, pH 7.9, 137 mM NaCl, 10 mM NaF, 1 mM EDTA, 1% Triton X-100, 0.2% Sarkosyl, and 10% glycerol) containing protease inhibitor cocktail (Sigma-Aldrich, St. Louis, MO, USA). Lysates were sonicated for 10 s and then incubated on ice for 30 min. Supernatants were collected by centrifuging at 12000 × g at 4°C for 30 min. The protein concentrations were measured using a BCA protein assay kit (23227, Pierce, Rockford, IL, USA). All of the protein samples were equalized for total protein after protein quantitation and subjected to 10% SDS/PAGE. Nitrocellulose membranes (GE Healthcare, Munich, Germany) were used to transfer the proteins via Western blotting. The membranes were blocked in 5% skim milk for 1 h at room temperature and then incubated overnight at 4°C with gentle shaking in diluted primary antibodies (1:500) against PSMD7 (sc-390705), Cyclin D1 (sc-450), Cyclin B1 (sc-7393), Cdk4 (sc-23896), Cdk1 (sc-54), Cdc25c (sc-13138), p53 (sc-126), p27 (sc-1641), p21 (sc-53870), Rb (sc-47562) (all obtained from Santa Cruz Biotechnology, Dallas, TX, USA), phospho-Rb (9308, Cell Signaling Technology, Danvers, MA, USA), caspase-3 (19677, Proteintech, Rosemont, IL, USA), cleaved caspase-3 (9661, Cell Signaling Technology, Danvers, MA, USA), and β-actin (A5441, Sigma-Aldrich). The membranes were incubated with horseradish peroxidase-labeled secondary antibodies after extensive washes and detected using an enhanced chemiluminescent kit (ECL, WBKLS-0500, Millipore, Bedford, MA, USA) with a ChemiDoc XRS (Bio-Rad, Hercules, CA, USA) detection system. The signals were analyzed and quantified via ImageJ software (National Institutes of Health, Bethesda, MD, USA) with β-actin as a loading control.

Immunohistochemistry (IHC)

The frozen tissues were sectioned at -20°C to a thickness of 10 μm and fixed in 4% paraformaldehyde for 15 min at room temperature. The slides were washed twice in phosphate-buffered saline (PBS) containing 0.3% Triton X-100 for 10 min each, followed by preincubation in 10% normal goat serum for 1 h. They were then washed 3 times with PBS and incubated overnight at 4°C with primary PSMD7 antibody at 1:100. Endogenous peroxidases were blocked with 0.3% H_2O_2 for 15 min. Biotinylated secondary antibody was added to the sections after extensive washing. Solutions containing streptavidin and biotin-conjugated HRP (Beyotime, China) was then added to the sections after washing 3 times. After incubation with the solution for 1 h, the sections were developed in 3'-diaminobenzidine (DAB, Beyotime, China) for 30 min after extensive washing. The reaction was stopped by rinsing in H_2O for 5 min. The sections were counterstained in hematoxylin, dehydrated, cleared, and mounted in neutral resin. A Leica upright microscope (DM4000B, Leica Microsystems, Heidelberg, Germany) was used to observe the immunohistochemical staining. For tissue microarray IHC staining, 4 μm paraffin embedded tissue sections were stained with PSMD7 primary antibody at a dilution of 1:25 after deparaffinization and antigen retrieval. The protein staining percentage was scored from 0 to 3 for each section. A score of 0 was given to samples with no positive cells or a percentage of positive cells ≤5%. A score of 1 was given to cases whose percentage of positive cells was 6%-25%. If the average percentage of positive cells

was >25% but ≤50%, then the expression was scored as 2, whereas the percentage of positive cells >50% but ≤75% was scored as 3. Finally, >75% positive staining percentage was scored as 4. Protein staining density was scored from 0 to 2 as follows: no staining was scored as 0, light brown as 1 and dark brown as 2. The final scores were calculated as the product of the staining percentage and intensity scores for each section. All of the sections were independently assessed by two pathologists. A mean score was used if controversial results were obtained.

siRNA transfection

siRNA duplexes targeting PSMD7 mRNA and one negative control scramble sequence were designed and synthesized to knock down the expression of target genes. MCF-7 and MDA-MB-231 cells were transfected by an Amaxa Cell Line Nucleofector Kit V (VCA-1003, Lonza, Cologne, Germany) according to the manufacturer's instructions. The specific sequences of the siRNAs were as follows: siPSMD7-1: 5'-GCCCUAAACUACACAAGAAUU-3' and 5'-UUCUUGUGUAGUUUAGGGCUU-3'; siPSMD7-2: 5'-UGACAUUGCCAUCAACGAAUU-3' and 5'-UUCGUUGAUGGCAAUGUCAUU-3'; and NC: 5'-UUCUCCGAACGUGUCACGUTT-3' and 5'-ACGUGACACGUUCGGAGAATT-3'.

Cell proliferation analysis

Cell proliferation assays were conducted using a kit containing WST-8 (CCK-8, CK04, Dojindo, Kumamoto, Japan). MCF-7 and MDA-MB-231 cells were seeded in 96-well plates at 1,500 cells per well after siRNA transfection. Cell proliferation was detected over the next 4 days following the manufacturer's protocol. The absorbance of each well was measured at 450 nm as the optical density (OD) of CCK-8 under a microplate reader (Bio-Rad Laboratories). The results were analyzed and are shown as the mean ± SD.

Cell viability

A crystal violet assay was used to measure the cell viability after siRNA transfection in breast cancer cells. MCF-7 and MDA-MB-231 cells were seeded in 6-well plates at a density of 50,000 cells per well after transfection. The cells were fixed with methanol and then stained with 0.1% crystal violet for a specific time. Various time points were selected to compare and show the difference. MCF-7 cells were stained on the third day, while MDA-MB-231 cells were stained on the fifth day after siRNA transfection.

Flow cytometric analysis

MCF-7 and MDA-MB-231 cells were harvested 72 h after transfection. Both floating and adherent cells were collected using centrifugation at 1200 × g for 10 min. Then, 70% ice cold ethanol diluted with PBS was used to fix the cells. The cells were stained with PI/RNase staining buffer (BD Biosciences, San Diego, CA, USA) and incubated at 37°C for 30 min. A Navios Flow Cytometer (Beckman Coulter, Brea, CA, USA) was used to analyze the results.

Senescence-associated β-galactosidase (SA-β-Gal) assay

Senescent cells were detected using a SA-β-Gal assay kit (C0602, Beyotime, Nantong, China) 72 h after transfection in accordance with the manufacturer's instructions. Specific cells stained by β-galactosidase were viewed under an inverted fluorescence microscope (DMI4000B, Leica Microsystems). Representative areas were captured under different conditions. The SA-β-Gal-positive senescent cells were calculated and expressed as a percentage of the total number of cells in five separate fields. Two independent experiments were conducted to calculate the average value and standard deviation of the SA-β-Gal-positive cells.

Quantitative RT-PCR (real-time PCR)

Total RNA was extracted from the harvested cells with TRIzol reagent (Invitrogen, Carlsbad, CA, USA) according to the manufacturer's protocol. Subsequently, cDNAs were synthesized using a Thermo Scientific RevertAid H Minus First Strand cDNA Synthesis kit (K1632, Thermo Fisher, Waltham, MA, USA). RT-PCR was performed on a QuantStudio Dx Real-Time PCR instrument (Applied Biosystems) using standard SYBR Green Master Mix (Applied Biosystems, Foster City, CA, USA) following the following cycle conditions: 10 min at 95°C followed by 40 cycles of 95°C for 15 s and 60°C for 1 min. The results were analyzed by the comparative cycle threshold method, and β-actin was used as an internal control. The sequences of primers (Sangon, Shanghai, China)

were as follows: PSMD7 F: 5'-TTGGAGCAGAGGAAGCTGAG-3', R: 5'-CTGACATCTGGCAGCAGGTT-3'; Cyclin D1, F: 5'-ACGAAGGTCTGCGCGTGTT-3', R: 5'-CCGCTGGCCATGAACTACCT-3'; Cdk4, F: 5'-CCTGGCCAGAATCTACAGCTA-3', R: 5'-ACATCTCGAGGCCAGTCATC-3'; Cyclin B1, F: 5'-AAGAGCTTTAAACTTTGGTCTGGG-3', R: 5'-CTTTGTAAGTCCTTGATTTACCATG-3'; Cdk1, F: 5'-TGGATCTGAAGAAATACTTGGATTCTA-3', R: 5'-CAATCCCCTGTAGGATTTGG-3'; Cdc25C, F: 5'-GATGTCCCTAGAACTCCAGTG-3', R: 5'-AGTTATCTCCCCACTGCTAAGA-3'; Rb, F: 5'-AGGATCAGATGAAGCAGATGG-3', R: 5'-TGCATTCGTGTTCGAGTAGAAG-3'; p21, F: 5'-CCATGTGGACCTGTCACTGTCTT-3', R: 5'-CGGCCTCTTGGAGAAGATCAGCCG-3'; p27, F: 5'-TTTGACTTGCATGAAGAGAAGC-3', R: 5'-AGCTGTCTCTGAAAGGGACATT-3' and β-actin, F: 5'-AGAGCTACGAGCTGCCTGAC-3', R: 5'-AGCACTGTGTTGGCGTACAG-3'.

P21 and p27 stability assay

MCF-7 cells were treated with 50 μg/ml cycloheximide (CHX) to block protein synthesis 48 h after transfection. The cells were harvested at specific time points and the p21 and p27 levels were determined via Western blotting. β-Actin was used as an internal reference.

Statistical analysis

The data are shown as the mean ± SD. ImageJ (version 1.8.0_112), GraphPad Instat software (GraphPad Prism 5.01, GraphPad Software Inc., San Diego, CA, USA), and SPSS statistics 17.0 were used to conduct the statistical analysis. The results were calculated by Student's t-test for comparisons between two groups and one-way ANOVA for multiple groups. Chi-squared or Fisher's exact test was used to analyze the correlation between PSMD7 and demographic and clinical features. Survival curves were compared using the log-rank test. Univariate and multivariate Cox regression were also used for survival analysis. A P value <0.05 was considered statistically significant.

Results

PSMD7 expression is upregulated in breast cancer tissues

PSMD7 is a key functional component of the 26S proteasome for protein degradation. To explore PSMD7 expression in breast cancer, we conducted an IHC analysis using tissue microarrays in a cohort of IDC patients. IHC staining data from 3 patients was missing from the microarray. PSMD7 expression was detected in both tumor and paired noncancerous tissues from 42 breast cancer patients (**Figures 1A** and S1). The results demonstrated that PSMD7 expression was upregulated in 40 (95.2%), unchanged in 1 (2.4%) and downregulated in 1 (2.4%) out of 42 patients. Thus, the PSMD7 level was significantly elevated in breast cancer tissues compared with noncancerous tissues ($P<0.001$, chi-squared test; **Figure 1B**). PSMD7 staining was observed in both the cytoplasm and nucleus in cells from tumor and noncancerous tissues. Stronger staining was detected in acinar cells and epithelial cells, and weaker staining was observed in fibroblasts and fat cells from the noncancerous tissues. PSMD7 staining in the tumor cells was much stronger than that in the controls. We also used frozen tissues from another cohort of 8 patients to perform IHC staining and Western blot analysis. PSMD7 staining was consistently stronger in the tumor tissues than in the controls (Figure S2). PSMD7 expression increased in 6 of 8 tumor tissues in comparison with the controls, as demonstrated by Western blotting (**Figure 1C**).

PSMD7 level is associated with clinical features and prognosis in breast cancer

We searched the TCGA database to analyze the relationship between the expression of PSMD7 and demographic and clinicopathological characteristics. The results showed that PSMD7 expression was associated with age, tumor subtype, tumor size, lymph node invasion, and tumor TNM stage (**Table 1**). A higher level of PSMD7 indicated a more progressive disease status in breast cancer. To explore the prognostic significance of PSMD7 expression in breast cancer patients, we conducted a long-term outcome analysis by data mining in the TCGA database. Our results demonstrated that patients with higher PSMD7 expression showed a significantly poorer OS and DFS compared to patients with a lower PSMD7 expression level (**Figure 2**). Furthermore, tumor subtype, lymph node invasion, distant metastasis, TNM stage, and PSMD7 expression were statistically associated with OS in the univariate Cox regression analysis. The multivariate Cox regression analy-

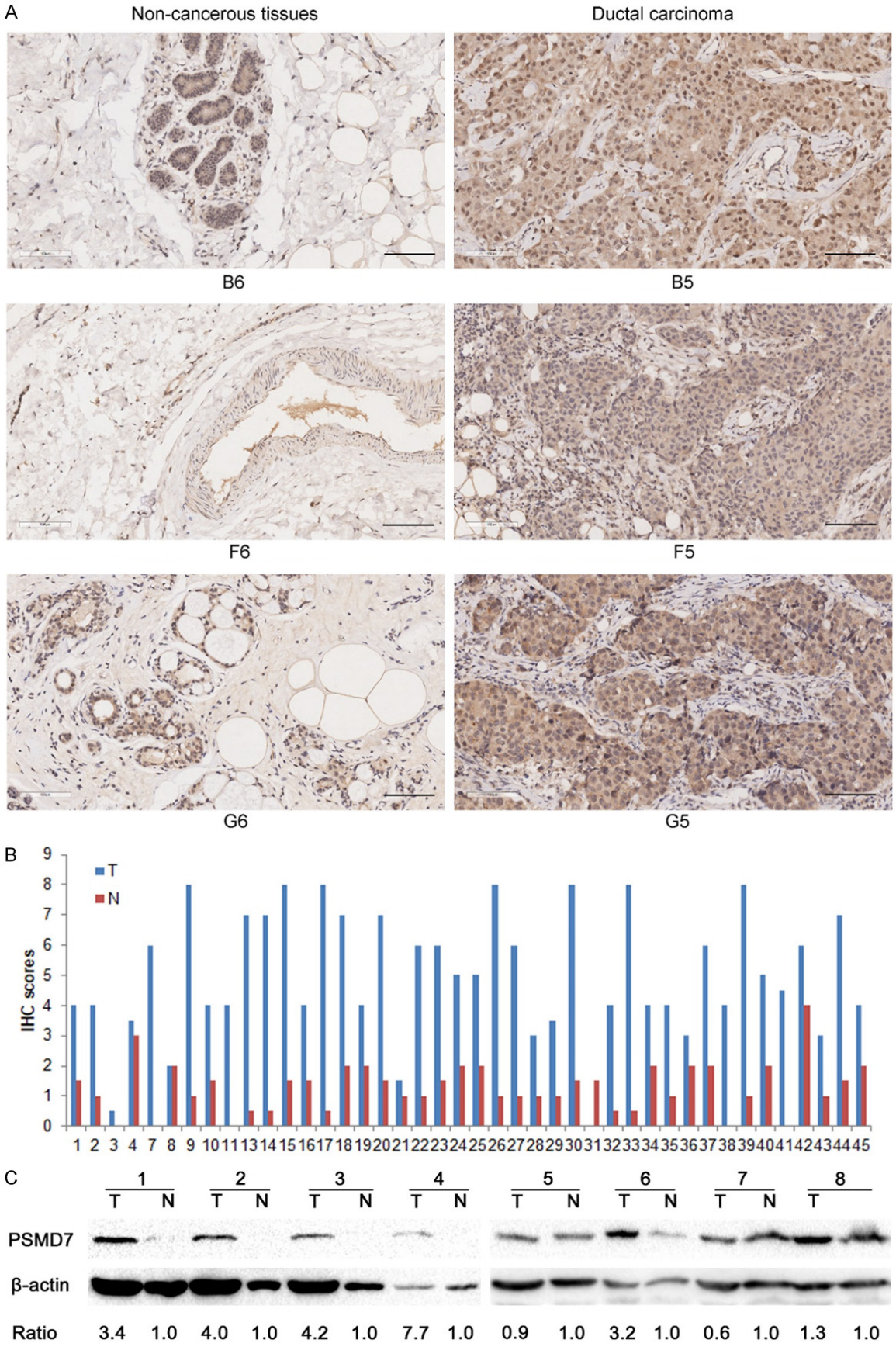
A
Non-cancerous tissues
Ductal carcinoma
B6
B5
F6
F5
G6
G5
B
T
N
IHC scores
0 1 2 3 4 5 6 7 8 9
1 2 3 4 7 8 9 10 11 13 14 15 16 17 18 19 20 21 22 23 24 25 26 27 28 29 30 31 32 33 34 35 36 37 38 39 40 41 42 43 44 45
C
1 2 3 4 5 6 7 8
T N T N T N T N T N T N T N T
PSMD7
β-actin
Ratio
3.4 1.0 4.0 1.0 4.2 1.0 7.7 1.0 0.9 1.0 3.2 1.0 0.6 1.0 1.3 1.0

Figure 1. PSMD7 expression is upregulated in breast cancer tissues. A. Typical IHC staining of PSMD7 in paired tumor and adjacent noncancerous tissues. IHC staining was performed in 45 pairs of tissues, and a representative image of three pairs is shown. The bar represents 100 μm. B. PSMD7 expression by IHC staining from a tissue microarray was scored in 42 pairs of breast cancer tissues (T) and adjacent noncancerous tissues (N) as referenced in the Materials and Methods section. Three pairs of tissues (A9 and A10; A11 and A12; B11 and B12) were excluded from the analysis due to missing staining data. C. PSMD7 protein expression in 8 paired tumor and adjacent noncancerous tissues from breast cancer patients was determined by Western blotting. β-Actin was used as an internal control. IHC: immunohistochemistry.

Table 1. The expression of PSMD7 correlated with demographic and clinical pathological characteristics in breast cancer patients

	PSMD7 High	PSMD7 Low	*P* value
Age			
≥50	372	417	0.002*
<50	169	124	
Prior malignancy history			
Yes	22	35	0.102
No	518	506	
Tumor subtype			
Normal	17	19	<0.001*
LumA	137	362	
LumB	117	80	
HER2	67	11	
Basal	153	18	
Tumor size			
T1	116	160	0.002*
T2-T4	424	379	
Lymph node invasion			
Negative	235	277	0.010*
Positive	296	254	
Distant metastasis			
Negative	445	449	0.332
Positive	16	11	
Tumor TNM stage			
I	67	113	<0.001*
II-IV	464	419	
Radiation treatment			
Yes	212	214	0.818
No	47	45	

The clinical information from 1,082 breast cancer patients was retrieved from the cBioportal for the Cancer Genome Atlas (TCGA) database for correlation analysis. The chi-square test was used to compare differences; *P<0.05 was considered significant.

sis indicated that prior malignancy history, lymph node invasion, distant metastasis, and PSMD7 expression were independent prognostic factors of OS in these patients (**Table 2**). Age, lymph node invasion, distant metastasis, and PSMD7 expression were associated with DFS in the univariate Cox regression analysis. However, age was the only independent predictor of DFS in the multivariate model. Distant metastasis and PSMD7 expression showed a marginally significant difference for DFS in breast cancer (**Table 3**).

PSMD7 knockdown induces cell cycle arrest, senescence, and apoptosis in breast cancer cells

To investigate the effects of PSMD7 on the growth of breast cancer cells, we knocked down the expression of PSMD7 in both MCF-7 and MDA-MB-231 cell lines via siRNA interference. Cell proliferation was examined by CCK-8 assays on the next four consecutive days after siRNA transfection. The results showed that PSMD7 knockdown significantly inhibited cell proliferation in both cell lines (**Figure 3A**). We further confirmed the results using crystal violet staining, where PSMD7 knockdown cells showed significantly fewer colonies than the controls (**Figure 3B**). To further clarify the mechanisms involved in proliferation inhibition, we conducted a flow cytometric analysis by PI staining to detect the cycle profile after PSMD7 was knocked down in the cells. Our results demonstrated that PSMD7 knockdown induced cell cycle arrest at the G0/G1 phase in MCF-7 cells and led to a slight increase in the number of apoptotic cells (sub-G1 phase). Although cell apoptosis was markedly increased in MDA-MB-231 cells after PSMD7 knockdown, the proportion of cells in the G0/G1 phase remained unchanged (**Figure 3C**). Finally, we detected cell senescence via SA-β-Gal staining after PSMD7 knockdown. Both breast cancer cell lines were stained with SA-β-Gal 72 h after transfection. We found that the cell morphology changed from a spindle shape to an enlarged,

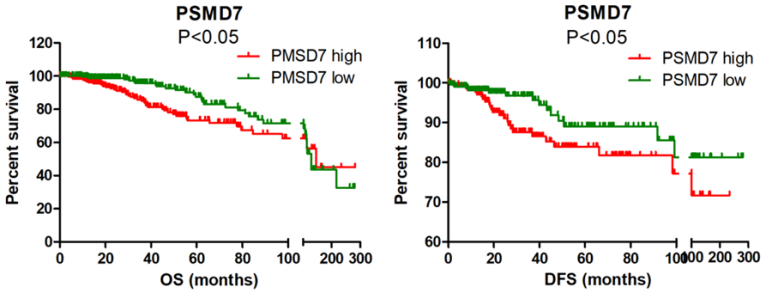

Figure 2. High PSMD7 expression indicates poor OS and DFS in breast cancer patients. Kaplan-Meier survival curves of upper and lower PSMD7 expression for OS and DFS in breast cancer patients. The patients were stratified into upper and lower quartiles for PSMD7 expression, resulting in 540 patients used for OS analysis and 464 patients for DFS analysis. The patient clinical information and PSMD7 expression were retrieved from the cBioportal for Cancer Genomics (TCGA) database and analyzed by a log-rank test. P<0.05 was considered statistically significant. OS: overall survival; DFS: disease-free survival.

flattened, and irregular shape after PSMD7 was knocked down in MCF-7 cells but not MDA-MB-231 cells (**Figure 4A**). PSMD7 knockdown induced a significant increase in the SA-β-Gal-positive cells among MCF-7 cells, whereas we did not observe obvious SA-β-Gal staining either in the controls or in PSMD7 knockdown MDA-MB-231 cells (**Figure 4A** and **4B**).

PSMD7 knockdown regulates the expression of cell cycle proteins

We investigated the underlying molecular mechanism by which PSMD7 regulates the cell cycle, apoptosis, and senescence in breast cancer cells. PSMD7 forms heterodimers with PSMD14 to modulate protein degradation in the 26S proteasome. Previous research demonstrated that PSMD14 knockdown inhibited cell growth by regulating cell cycle proteins [18]. Thus, disruption of the PSMD14-PSMD7 complex may have a profound effect on these proteins. We evaluated Cyclin D1, Cdk4, Cyclin B1, Cdk1, Cdc25c, p27, p21, Rb, pRb, caspase-3, and cleaved caspase-3 protein expression after PSMD7 was depleted from breast cancer cells. Our analysis demonstrated that the expression of the cell cycle proteins Cyclin D1, Cdk4, Cyclin B1, Cdk1, and Cdc25c was significantly reduced in MCF-7 cells, whereas the expression of Cdk1 and Cdc25c was decreased in MDA-MB-231 cells when PSMD7 was knocked down (**Figure 5A**). Moreover, p27 and p21 levels were markedly increased in both cell lines, whereas cleaved caspase-3 showed a slight increase in MCF-7 cells and a dramatic increase in MDA-MB-231 cells (**Figure 5A**). Additionally, the levels of Rb and pRb showed a significant reduction in both cell lines (**Figure 5A**). To examine whether the knockdown of PSMD7 affects the transcriptional regulation of the cell cycle proteins, the mRNA expression of these proteins was also determined after PSMD7 was knocked down in both cell lines. The results indicated that the mRNA levels of Cyclin D1, Cdk4, Cyclin B1, Cdk1, and Cdc25c were significantly reduced 48 to 72 h after PSMD7 knockdown in both cell lines (**Figure 5B** and **5C**), suggesting that PSMD7 may play a role in transcriptional repression. Although p21 and p27 protein levels were markedly elevated after PSMD7 silencing, we did not observe an increase in p21 or p27 mRNA expression in either cell type (**Figure 5**).

PSMD7 knockdown increases the stability of p21 and p27

P21 and p27 are the founding members of the Cip/Kip family of CKIs, which regulate cell cycle progression and cell senescence [19-23]. The stability of both proteins is regulated by ubiquitination and proteasome-mediated degradation [24]. Depletion of PSMD7 may cause proteasome malfunction, so it is of interest to explore whether knockdown of PSMD7 affects the stability of p21 and p27. We blocked protein synthesis using CHX 48 h after transfection and harvested the cells at a series of specific time points. PSMD7 was effectively knocked down by the siRNA sequence after transfection. The PSMD7 level remained steady even after the cells were treated with CHX for 5 h (**Figure 6A**). P21 and p27 protein expression gradually and markedly decreased after CHX treatment. Importantly, the stability of both proteins significantly increased after PSMD7 knockdown in breast cancer cells in comparison with that of the controls (**Figure 6A** and **6B**). These results suggested that disruption of the proteasome by depleting PSMD7 may have a

Table 2. Univariate and multivariate Cox regression analyses of prognostic factors of overall survival (OS) in breast cancer patients

Parameters	n	Univariate regression analysis		Multivariate regression analysis (n=363)	
		HR (95% CI)	*P* value	HR (95% CI)	*P* value
Age	502	1.328 (0.786-2.244)	0.289	-	-
Prior malignancy history	501	2.246 (0.893-5.644)	0.085	3.945 (1.104-14.094)	0.035*
Tumor subtype	452		0.097		0.978
LumA		1.250 (0.159-9.799)	0.832	0.000 (0.000-1.057E+278)	0.974
LumB		1.162 (0.571-2.363)	0.679	1.202 (0.418-3.457)	0.733
HER2		1.331 (0.539-3.288)	0.536	1.002 (0.338-2.970)	0.997
Basal		3.007 (1.243-7.274)	0.015*	1.410 (0.424-4.691)	0.575
Tumor size	501	1.276 (0.749-2.175)	0.369	-	-
Lymph node invasion	491	2.933 (1.725-4.988)	<0.001*	2.652 (1.157-6.084)	0.021
Distant metastasis	426	7.700 (3.629-16.341)	<0.001*	5.832 (2.239-15.190)	<0.001*
TNM stage	494	2.220 (1.060-4.647)	0.034*	1.483 (0.389-5.654)	0.564
Radiation treatment	478	0.653 (0.393-1.084)	0.099	0.556 (0.289-1.073)	0.080
PSMD7 expression	502	1.205 (1.056-1.375)	0.006*	1.310 (1.038-1.652)	0.023*

Data from a total of 540 breast cancer patients with demographic and clinical information were extracted from the cBioportal for Cancer Genomics (TCGA) database for univariate and multivariate Cox regression analyses. Normal subtype was used as a contrast indicator (reference category). HR: hazard ratio, CI: confidence interval. *P<0.05 was considered significant.

Table 3. Univariate and multivariate Cox regression analyses of prognostic factors of disease-free survival (DFS) in breast cancer patients

Parameters	n	Univariate regression analysis		Multivariate regression analysis (n=369)	
		HR (95% CI)	*P* value	HR (95% CI)	*P* value
Age	449	0.435 (0.232-0.816)	0.010*	0.367 (0.180-0.746)	0.006*
Prior malignancy history	448	1.168 (0.280-4.872)	0.832	-	-
Tumor subtype	407		0.939	-	-
LumA		0.000 (0.000-3.213E+302)	0.975	-	-
LumB		0.851 (0.367-1.972)	0.706	-	-
HER2		0.628 (0.189-2.089)	0.449	-	-
Basal		1.134 (0.300-4.289)	0.854	-	-
Tumor size	449	1.740 (0.799-3.788)	0.163	-	-
Lymph node invasion	444	2.130 (1.077-4.215)	0.030*	1.288 (0.594-2.792)	0.521
Distant metastasis	373	9.585 (1.293-71.046)	0.027*	6.442 (0.794-52.244)	0.081
TNM stage	445	2.564 (0.907-7.242)	0.076	2.254 (0.621-8.184)	0.217
Radiation treatment	430	0.897 (0.476-1.690)	0.736	-	-
PSMD7 expression	449	1.197 (1.002-1.430)	0.048*	1.227 (0.996-1.511)	0.054

Data from a total of 464 breast cancer patients with demographic and clinical information were extracted from the cBioportal for Cancer Genomics (TCGA) database for univariate and multivariate Cox regression analyses. The normal subtype was used as a contrast indicator (reference category). HR: hazard ratio, CI: confidence interval. *P<0.05 was considered significant.

profound effect on the stability of cell cycle proteins.

Discussion

Breast cancer remains one of the most serious public health issues worldwide. With an annual incidence of more than 500,000 deaths, breast cancer is the most common cause of cancer-related death in women [25]. Although new drugs and treatment regimens have significantly relieved disease progression, a number of patients showed a poor prognosis and a higher risk of disease relapse [26]. Conducting personalized therapies on specific molecular subtypes is of considerable value [27]. Thus, iden-

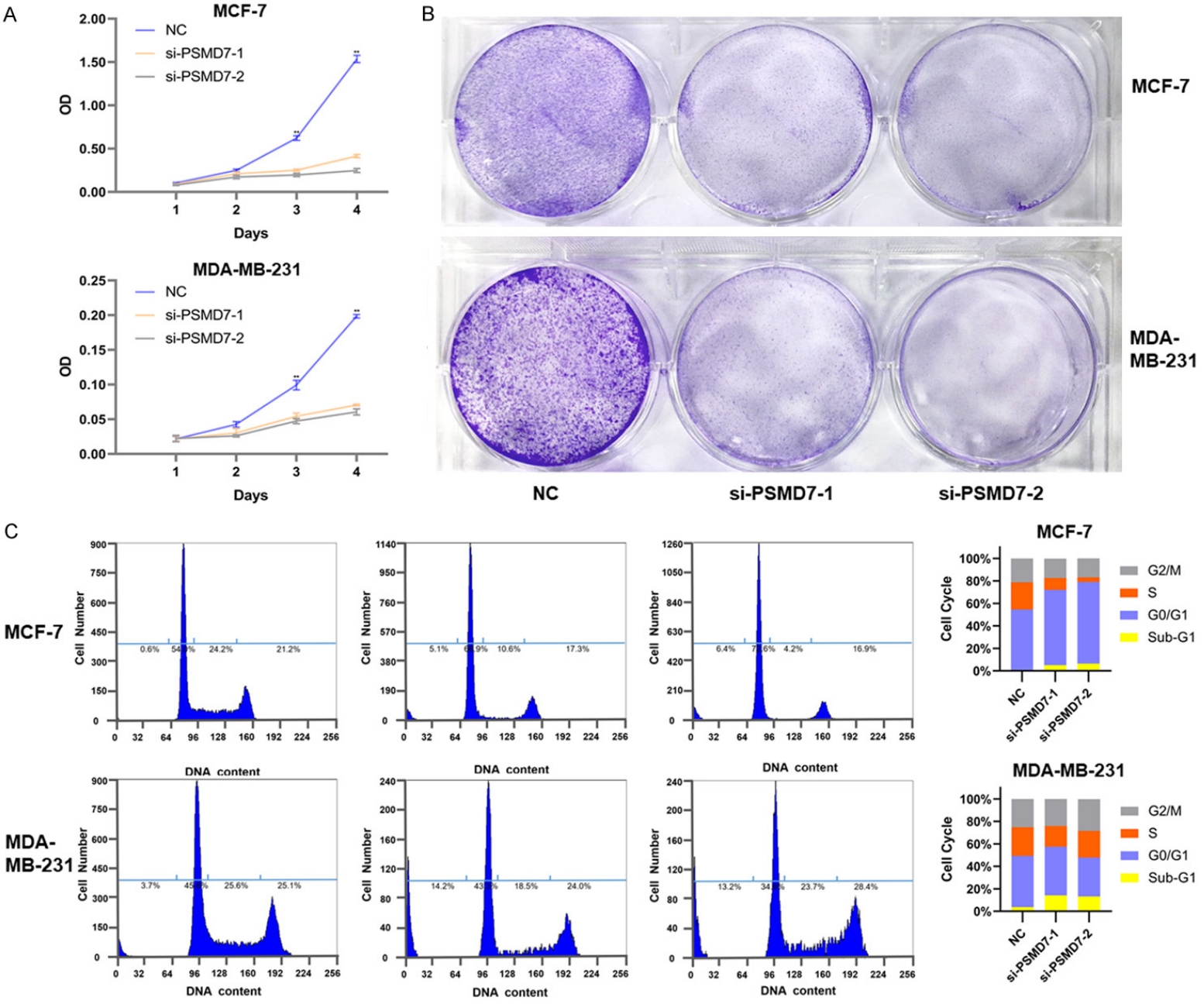
A
MCF-7
NC
si-PSMD7-1
si-PSMD7-2
OD
Days
MDA-MB-231
B
MCF-7
MDA-MB-231
NC
si-PSMD7-1
si-PSMD7-2
C
MCF-7
MDA-MB-231
Cell Number
DNA content
Cell Cycle
G2/M
S
G0/G1
Sub-G1

Figure 3. PSMD7 knockdown induces cell cycle arrest and apoptosis in breast cancer cells. A. The viability of MCF-7 and MDA-MB-231 cells transfected with NC and two siRNA sequences against PSMD7 (si-PSMD7-1 and si-PSMD7-2) was assessed by CCK-8 assays. The OD value was determined at 1, 2, 3 and 4 days post-transfection. The assays were performed at four replicates for each group. The experiments were repeated twice, and a representative result is shown. B. Crystal violet staining was conducted to assess the survival of MCF-7 and MDA-MB-231 cells transfected with NC, si-PSMD7-1 or si-PSMD7-2 for 72 hours. The experiments were repeated twice, and a representative staining is shown. C. MCF-7 and MDA-MB-231 cells were treated with NC, si-PSMD7-1 or si-PSMD7-2 for 72 hours. Cell cycle and apoptosis (sub-G1 phase) were determined by PI staining followed by FACS analysis (left panel). The percentage of cells in each phase of the cell cycle is also demonstrated (right panel). The experiments were repeated twice, and a representative result is shown. **represents P<0.01 by Student's t-test. NC: scrambled control siRNA; PI: propidium iodide.

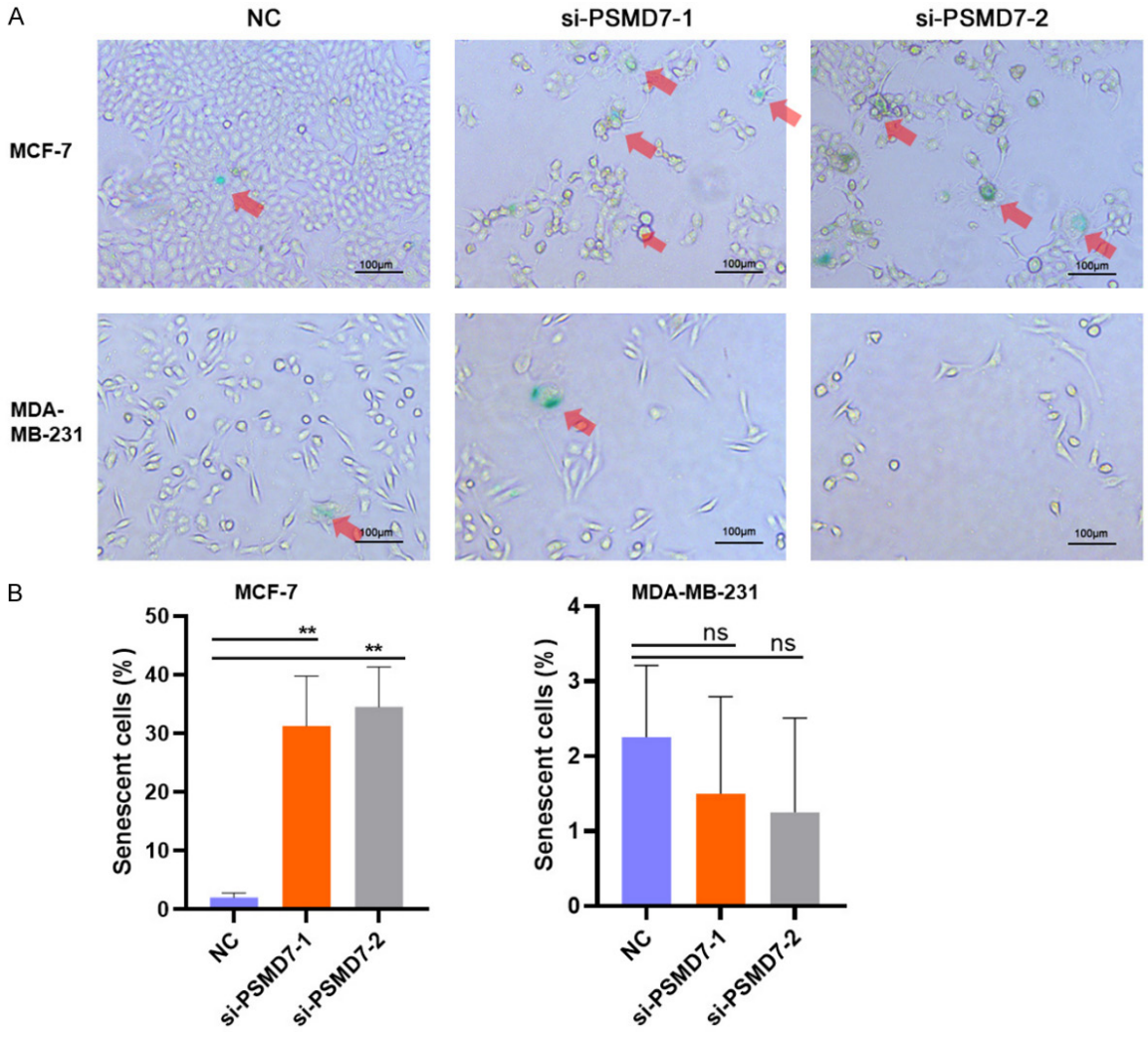

Figure 4. PSMD7 knockdown induces cellular senescence in MCF-7 but not MDA-MB-231 cells. A, B. Exponentially growing MCF-7 and MDA-MB-231 cells were transfected with NC, si-PSMD7-1 or si-PSMD7-2. After 72 hours, the cells were fixed and incubated with SA-β-Gal staining solution overnight. The senescence-like phenotype was imaged by microscopy (100-fold). The number of SA-β-Gal-positive cells was counted and is expressed as a percentage of the total number of cells in five separate fields. The means and standard deviation of SA-β-Gal-positive cells were derived from two independent experiments. **represents P<0.01 by Student's t-test; ns: not significant. SA-β-Gal: senescence-associated β-galactosidase.

tifying and evaluating new biomarkers and therapeutic targets is a high priority. We found that PSMD7 was significantly upregulated in breast cancer tissues. A high PSMD7 level was associated with a worse tumor subtype, larger tumor size, lymph node invasion, and advanced

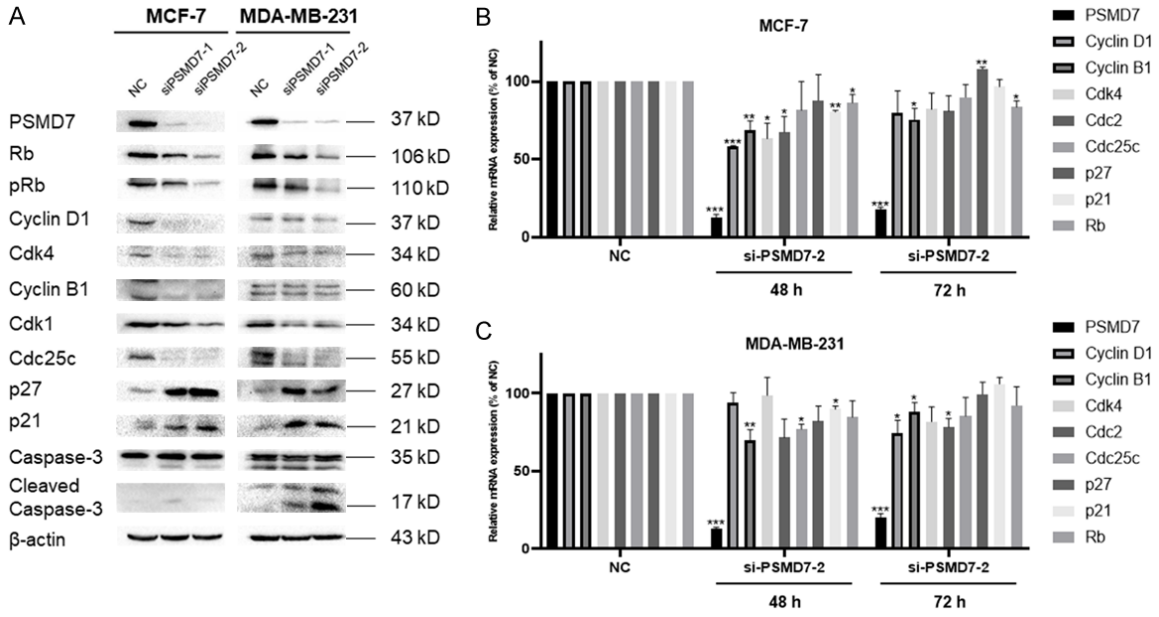

Figure 5. A. Whole-cell lysates from MCF-7 and MDA-MB-231 cells were extracted after the cells were transfected with NC, si-PSMD7-1 or si-PSMD7-2 for 72 hours. Aliquots of 30 μg whole-cell lysates were subjected to SDS-PAGE followed by Western blot analysis of the indicated antibodies. β-Actin was used as a loading control. B, C. MCF-7 and MDA-MB-231 cells were transfected with NC or si-PSMD7-2 for 48 and 72 hours. The mRNA expression of cell cycle-related proteins was detected by RT-PCR. *P* values were calculated by Student's t-test (*P<0.05, **P<0.01, and ***P<0.001). NC: scrambled control siRNA; RT-PCR: real-time PCR.

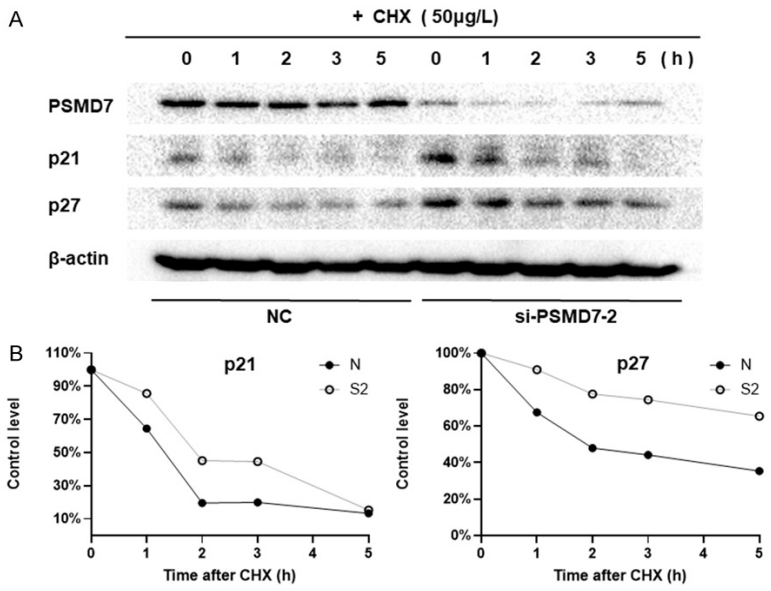

Figure 6. Knockdown of PSMD7 promotes p21 and p27 stability in breast cancer cells. A. MCF-7 cells were transfected with NC or si-PSMD7-2. After 24 hours, cells were treated with 50 μg/ml CHX and collected at the indicated time points. Western blot analysis was performed with p21, p27 and PSMD7 antibodies. β-Actin was used as an internal control. B. Quantification of the p21 and p27 levels relative to β-actin expression at indicated time points was determined by ImageJ software, and the degradation curve is shown. NC: scrambled control siRNA; CHX: cycloheximide.

TNM stage. The increased PSMD7 expression in tumor tissues predicted poor OS and DFS in breast cancer patients. Thus, PSMD7 may be a potential prognostic marker for breast cancer patients.

Proteasome inhibitors have recently shown significant anticancer value [28-32]. PSMD7 and PSMD14 are the core components of the 26S proteasome and are closely connected. PSMD7 interacts with PSMD14 to activate proteasome function to regulate ubiquitinated substrate degradation. Although many studies have demonstrated that PSMD14 is an antiproteasome target for tumor therapies of different cancer types [11, 12], the role and function of PSMD7 in tumorigenesis remains largely unknown. We

found that knockdown of PSMD7 inhibited cell proliferation by inducing cell cycle arrest, senescence, and apoptosis in breast cancer cells. PSMD7 knockdown mainly induced G1 phase arrest and senescence in MCF-7 cells but promoted cell apoptosis in MDA-MB-231 cells, suggesting that the effects of PSMD7 on cell growth and survival were cell-type specific. The absence of p53 may result in a reduction in DNA damage repair and directly lead to cell apoptosis in MDA-MB-231 cells. In fact, we observed a slight increase in apoptotic cells in MCF-7 cells. The cleaved caspase 3 level was consistently elevated after PSMD7 was depleted in both cell lines. Further investigation is needed to clarify the underlying molecular events by which PSMD7 regulates cell apoptosis.

Cell cycle progression is tightly regulated by cyclins, cyclin-dependent kinases (Cdks), and Cdk inhibitors. Cyclin D/Cdk4 regulates the transition from the G1 phase to the S phase, whereas Cyclin B/Cdk1 regulates the transition from the G2 phase to the M phase [33-35]. Rb, a G1 phase cell cycle inhibitor, is phosphorylated and activated, which disables the inhibition of transcription factors and allows the transcription of cell cycle genes, thus promoting the transition of cells from the G1 phase to the S phase. Cdc25c (cell division cycle 25), a tyrosine phosphatase dephosphorylated Cdk1, triggers mitosis [36, 37]. We observed that both the mRNA and protein levels of these cell cycle-related proteins were markedly inhibited in PSMD7 knockdown cells, suggesting that PSMD7 may regulate gene transcription in a direct or indirect manner.

P21 and p27 are members of the Cdk inhibitor (CKI) family and negatively regulate the cell cycle [38, 39]. P21 and p27 inhibit Cdk activity and induce cell cycle arrest, senescence, and apoptosis in response to various stimuli [40-43]. Both proteins are involved in tumor progression in breast cancer [44]. We determined that p21 and p27 significantly increased after PSMD7 was knocked down in breast cancer cells, implying that PSMD7-mediated CKI regulation may play a critical role in the tumorigenesis of breast cancer. Previous studies indicated that p21 and p27 caused Rb dephosphorylation and depletion [45]. We observed a consistent increase in p21 and p27 levels and a concomitant decrease in Rb and pRb in PSMD7-depleted cells. Although PSMD7 knockdown inhibited gene transcription, we found that elevated p21 and p27 levels were the result of the increased stability of both proteins. Previous studies indicated that the degradation of both proteins was highly dependent on an intact proteasome [46, 47]. Depletion of PSMD7 may disrupt the proteasome, leading to malfunction of the protein degradation pathway in cells.

Conclusions

In summary, our results showed that the PSMD7 level was significantly upregulated in breast cancer tissues and closely related to clinical features. A higher PSMD7 level was associated with progressive disease and predicted poor survival in breast cancer patients. Knockdown of PSMD7 induced cell cycle arrest, senescence, and apoptosis by regulating cell cycle proteins in breast cancer cells. Our results indicate that PSMD7 may be a strong prognostic indicator and potential therapeutic target for breast cancer.

Acknowledgements

This study was supported by the National Natural Science Foundation of China (81972624), Suzhou Science and Technology Development Program (SYSD2019001), and the Research Foundation for Advanced Talents by the Affiliated Zhangjiagang Hospital of Soochow University (ZKY201900) to Dawei Li.

Disclosure of conflict of interest

None.

Abbreviations

PSMD7, proteasome 26S subunit, non-ATPase 7; Rb, retinoblastoma protein; Cdks, cyclin-dependent kinases; CKI, Cdk inhibitor; OS, overall survival; DFS, disease-free survival; TCGA, The Cancer Genome Atlas; DMEM, Dulbecco's Modified Eagle Medium; FBS, fetal bovine serum; PI, propidium iodide; SA-β-Gal, senescence-associated β-galactosidase; RT-PCR, real-time PCR; CHX, cycloheximide; ECL, enhanced chemiluminescence; IHC, immunohistochemistry; PBS, phosphate-buffered saline.

Address correspondence to: Dawei Li, Center for Translational Medicine, Affiliated Zhangjiagang Hos-

pital of Soochow University, #68 Jiyang West Road, Suzhou 215600, Jiangsu, China. E-mail: daweili@suda.edu.cn; Shusheng Wang, Department of General Surgery, Affiliated Zhangjiagang Hospital of Soochow University, #68 Jiyang West Road, Suzhou 215600, Jiangsu, China. E-mail: drwangsszjg@163.com

References

[1] Bray F, Ferlay J, Soerjomataram I, Siegel RL, Torre LA and Jemal A. Global cancer statistics 2018: GLOBOCAN estimates of incidence and mortality worldwide for 36 cancers in 185 countries. CA Cancer J Clin 2018; 68: 394-424.

[2] Nguyen PL, Taghian AG, Katz MS, Niemierko A, Abi Raad RF, Boon WL, Bellon JR, Wong JS, Smith BL and Harris JR. Breast cancer subtype approximated by estrogen receptor, progesterone receptor, and HER-2 is associated with local and distant recurrence after breast-conserving therapy. J Clin Oncol 2008; 26: 2373-2378.

[3] Lehmann BD, Bauer JA, Chen X, Sanders ME, Chakravarthy AB, Shyr Y and Pietenpol JA. Identification of human triple-negative breast cancer subtypes and preclinical models for selection of targeted therapies. J Clin Invest 2011; 121: 2750-2767.

[4] Pathare GR, Nagy I, Sledz P, Anderson DJ, Zhou HJ, Pardon E, Steyaert J, Forster F, Bracher A and Baumeister W. Crystal structure of the proteasomal deubiquitylation module Rpn8-Rpn11. Proc Natl Acad Sci U S A 2014; 111: 2984-2989.

[5] Shah SA, Potter MW, McDade TP, Ricciardi R, Perugini RA, Elliott PJ, Adams J and Callery MP. 26S proteasome inhibition induces apoptosis and limits growth of human pancreatic cancer. J Cell Biochem 2001; 82: 110-122.

[6] Jacquemont C and Taniguchi T. Proteasome function is required for DNA damage response and fanconi anemia pathway activation. Cancer Res 2007; 67: 7395-7405.

[7] McBride A and Ryan PY. Proteasome inhibitors in the treatment of multiple myeloma. Expert Rev Anticancer Ther 2013; 13: 339-358.

[8] Dubiel W, Ferrell K, Dumdey R, Standera S, Prehn S and Rechsteiner M. Molecular cloning and expression of subunit 12: a non-MCP and non-ATPase subunit of the 26 S protease. FEBS Lett 1995; 363: 97-100.

[9] Tsurumi C, DeMartino GN, Slaughter CA, Shimbara N and Tanaka K. cDNA cloning of p40, a regulatory subunit of the human 26S proteasome, and a homolog of the Mov-34 gene product. Biochem Biophys Res Commun 1995; 210: 600-608.

[10] Zhang L, Xu H, Ma C, Zhang J, Zhao Y, Yang X, Wang S and Li D. Upregulation of deubiquitinase PSMD14 in lung adenocarcinoma (LUAD) and its prognostic significance. J Cancer 2020; 11: 2962-2971.

[11] Zhu R, Liu Y, Zhou H, Li L, Li Y, Ding F, Cao X and Liu Z. Deubiquitinating enzyme PSMD14 promotes tumor metastasis through stabilizing SNAIL in human esophageal squamous cell carcinoma. Cancer Lett 2018; 418: 125-134.

[12] Luo G, Hu N, Xia X, Zhou J and Ye C. RPN11 deubiquitinase promotes proliferation and migration of breast cancer cells. Mol Med Rep 2017; 16: 331-338.

[13] Shi K, Zhang JZ, Zhao RL, Yang L and Guo D. PSMD7 downregulation induces apoptosis and suppresses tumorigenesis of esophageal squamous cell carcinoma via the mTOR/p70S6K pathway. FEBS Open Bio 2018; 8: 533-543.

[14] Mahalingam S, Ayyavoo V, Patel M, Kieber-Emmons T, Kao GD, Muschel RJ and Weiner DB. HIV-1 Vpr interacts with a human 34-kDa mov34 homologue, a cellular factor linked to the G2/M phase transition of the mammalian cell cycle. Proc Natl Acad Sci U S A 1998; 95: 3419-3424.

[15] Niu Z, Lei R, Shi J, Wang D, Shou W, Wang Z, Wang Y, Wang Z and Huang W. A polymorphism rs17336700 in the PSMD7 gene is associated with ankylosing spondylitis in Chinese subjects. Ann Rheum Dis 2011; 70: 706-707.

[16] Cerami E, Gao J, Dogrusoz U, Gross BE, Sumer SO, Aksoy BA, Jacobsen A, Byrne CJ, Heuer ML, Larsson E, Antipin Y, Reva B, Goldberg AP, Sander C and Schultz N. The cBio cancer genomics portal: an open platform for exploring multidimensional cancer genomics data. Cancer Discov 2012; 2: 401-404.

[17] Gao J, Aksoy BA, Dogrusoz U, Dresdner G, Gross B, Sumer SO, Sun Y, Jacobsen A, Sinha R, Larsson E, Cerami E, Sander C and Schultz N. Integrative analysis of complex cancer genomics and clinical profiles using the cBioPortal. Sci Signal 2013; 6: pl1.

[18] Byrne A, McLaren RP, Mason P, Chai L, Dufault MR, Huang Y, Liang B, Gans JD, Zhang M, Carter K, Gladysheva TB, Teicher BA, Biemann HP, Booker M, Goldberg MA, Klinger KW, Lillie J, Madden SL and Jiang Y. Knockdown of human deubiquitinase PSMD14 induces cell cycle arrest and senescence. Exp Cell Res 2010; 316: 258-271.

[19] Liang YC, Lin-Shiau SY, Chen CF and Lin JK. Inhibition of cyclin-dependent kinases 2 and 4 activities as well as induction of Cdk inhibitors p21 and p27 during growth arrest of human breast carcinoma cells by (-)-epigallocatechin-3-gallate. J Cell Biochem 1999; 75: 1-12.

[20] Albrecht JH, Poon RY, Ahonen CL, Rieland BM, Deng C and Crary GS. Involvement of p21 and p27 in the regulation of CDK activity and cell cycle progression in the regenerating liver. Oncogene 1998; 16: 2141-2150.
[21] Passos JF, Nelson G, Wang C, Richter T, Simillion C, Proctor CJ, Miwa S, Olijslagers S, Hallinan J, Wipat A, Saretzki G, Rudolph KL, Kirkwood TB and von Zglinicki T. Feedback between p21 and reactive oxygen production is necessary for cell senescence. Mol Syst Biol 2010; 6: 347.
[22] Alexander K and Hinds PW. Requirement for p27 (KIP1) in retinoblastoma protein-mediated senescence. Mol Cell Biol 2001; 21: 3616-3631.
[23] Collado M, Medema RH, Garcia-Cao I, Dubuisson ML, Barradas M, Glassford J, Rivas C, Burgering BM, Serrano M and Lam EW. Inhibition of the phosphoinositide 3-kinase pathway induces a senescence-like arrest mediated by p27Kip1. J Biol Chem 2000; 275: 21960-21968.
[24] Lu Z and Hunter T. Ubiquitylation and proteasomal degradation of the p21(Cip1), p27(Kip1) and p57(Kip2) CDK inhibitors. Cell Cycle 2010; 9: 2342-2352.
[25] Gingras I, Desmedt C, Ignatiadis M and Sotiriou C. CCR 20th anniversary commentary: gene-expression signature in breast cancer--where did it start and where are we now? Clin Cancer Res 2015; 21: 4743-4746.
[26] Kassam F, Enright K, Dent R, Dranitsaris G, Myers J, Flynn C, Fralick M, Kumar R and Clemons M. Survival outcomes for patients with metastatic triple-negative breast cancer: implications for clinical practice and trial design. Clin Breast Cancer 2009; 9: 29-33.
[27] Le Du F, Eckhardt BL, Lim B, Litton JK, Moulder S, Meric-Bernstam F, Gonzalez-Angulo AM and Ueno NT. Is the future of personalized therapy in triple-negative breast cancer based on molecular subtype? Oncotarget 2015; 6: 12890-12908.
[28] Oyaizu H, Adachi Y, Okumura T, Okigaki M, Oyaizu N, Taketani S, Ikebukuro K, Fukuhara S and Ikehara S. Proteasome inhibitor 1 enhances paclitaxel-induced apoptosis in human lung adenocarcinoma cell line. Oncol Rep 2001; 8: 825-829.
[29] Zhang Y, Shi Y, Li X, Du R, Luo G, Xia L, Du W, Chen B, Zhai H, Wu K and Fan D. Proteasome inhibitor MG132 reverses multidrug resistance of gastric cancer through enhancing apoptosis and inhibiting P-gp. Cancer Biol Ther 2008; 7: 540-546.
[30] Jones MD, Liu JC, Barthel TK, Hussain S, Lovria E, Cheng D, Schoonmaker JA, Mulay S, Ayers DC, Bouxsein ML, Stein GS, Mukherjee S and Lian JB. A proteasome inhibitor, bortezomib, inhibits breast cancer growth and reduces osteolysis by downregulating metastatic genes. Clin Cancer Res 2010; 16: 4978-4989.
[31] Ling YH, Liebes L, Jiang JD, Holland JF, Elliott PJ, Adams J, Muggia FM and Perez-Soler R. Mechanisms of proteasome inhibitor PS-341-induced G(2)-M-phase arrest and apoptosis in human non-small cell lung cancer cell lines. Clin Cancer Res 2003; 9: 1145-1154.
[32] Zhi T, Jiang K, Xu X, Yu T, Zhou F, Wang Y, Liu N and Zhang J. ECT2/PSMD14/PTTG1 axis promotes the proliferation of glioma through stabilizing E2F1. Neuro Oncol 2019; 21: 462-473.
[33] Baldin V, Lukas J, Marcote MJ, Pagano M and Draetta G. Cyclin D1 is a nuclear protein required for cell cycle progression in G1. Genes Dev 1993; 7: 812-821.
[34] Lange C, Huttner WB and Calegari F. Cdk4/cyclinD1 overexpression in neural stem cells shortens G1, delays neurogenesis, and promotes the generation and expansion of basal progenitors. Cell Stem Cell 2009; 5: 320-331.
[35] Takizawa CG and Morgan DO. Control of mitosis by changes in the subcellular location of cyclin-B1-Cdk1 and Cdc25C. Curr Opin Cell Biol 2000; 12: 658-665.
[36] Peng CY, Graves PR, Thoma RS, Wu Z, Shaw AS and Piwnica-Worms H. Mitotic and G2 checkpoint control: regulation of 14-3-3 protein binding by phosphorylation of Cdc25C on serine-216. Science 1997; 277: 1501-1505.
[37] Matsuoka S, Huang M and Elledge SJ. Linkage of ATM to cell cycle regulation by the Chk2 protein kinase. Science 1998; 282: 1893-1897.
[38] Toyoshima H and Hunter T. p27, a novel inhibitor of G1 cyclin-Cdk protein kinase activity, is related to p21. Cell 1994; 78: 67-74.
[39] Polyak K, Lee MH, Erdjument-Bromage H, Koff A, Roberts JM, Tempst P and Massague J. Cloning of p27Kip1, a cyclin-dependent kinase inhibitor and a potential mediator of extracellular antimitogenic signals. Cell 1994; 78: 59-66.
[40] Roy S, Kaur M, Agarwal C, Tecklenburg M, Sclafani RA and Agarwal R. p21 and p27 induction by silibinin is essential for its cell cycle arrest effect in prostate carcinoma cells. Mol Cancer Ther 2007; 6: 2696-2707.
[41] Mu C, Jia P, Yan Z, Liu X, Li X and Liu H. Quercetin induces cell cycle G1 arrest through elevating Cdk inhibitors p21 and p27 in human hepatoma cell line (HepG2). Methods Find Exp Clin Pharmacol 2007; 29: 179-183.
[42] Don MJ, Chang YH, Chen KK, Ho LK and Chau YP. Induction of CDK inhibitors (p21(WAF1) and p27(Kip1)) and Bak in the beta-lapachone-induced apoptosis of human prostate cancer cells. Mol Pharmacol 2001; 59: 784-794.
[43] Schwandner O, Bruch HP and Broll R. Prognostic significance of p21 and p27 protein, apop-

tosis, clinical and histologic factors in rectal cancer without lymph node metastases. Eur Surg Res 2002; 34: 389-396.

[44] Wong SC, Chan JK, Lee KC and Hsiao WL. Differential expression of p16/p21/p27 and cyclin D1/D3, and their relationships to cell proliferation, apoptosis, and tumour progression in invasive ductal carcinoma of the breast. J Pathol 2001; 194: 35-42.

[45] Broude EV, Swift ME, Vivo C, Chang BD, Davis BM, Kalurupalle S, Blagosklonny MV and Roninson IB. p21 (Waf1/Cip1/Sdi1) mediates retinoblastoma protein degradation. Oncogene 2007; 26: 6954-6958.

[46] Sheaff RJ, Singer JD, Swanger J, Smitherman M, Roberts JM and Clurman BE. Proteasomal turnover of p21Cip1 does not require p21Cip1 ubiquitination. Mol Cell 2000; 5: 403-410.

[47] Pagano M, Tam SW, Theodoras AM, Beer-Romero P, Del Sal G, Chau V, Yew PR, Draetta GF and Rolfe M. Role of the ubiquitin-proteasome pathway in regulating abundance of the cyclin-dependent kinase inhibitor p27. Science 1995; 269: 682-685.

Table S1. The demographic and clinicopathological features of 45 breast IDC patients from tissue microarray

Patient	Age	Gender	Pathological Stages	Primary tumor	Laterality	Tumor size	Lymph node invasion stage	Distant metastasis	TNM Stage	Tumor types
1	44	F	II-III	Yes	Left	Tis	N0	M0	0	Intraductal arcinoma
2	42	F	II	Yes	Left	Tis	N0	M0	0	Intraductal arcinoma
3	59	F	II-III	Yes	Right	T1	N0	M0	IA	Invasive carcinoma
4	48	F	II-III	Yes	Right+Left	T1	N0	M0	IA	Invasive carcinoma
5	84	F	II	Yes	Left	T1	N0	M0	IA	Invasive carcinoma
6	45	F	II-III	Yes	Right	T1	N0	M0	IA	Invasive carcinoma
7	52	F	III	Yes	Left	T2	N0	M0	IIA	Invasive carcinoma
8	40	F	II-III	Yes	Right	T2	N0	M0	IIA	Invasive carcinoma
9	46	F	II	Yes	Right	T2	N0	M0	IIA	Invasive carcinoma
10	60	F	I-II	Yes	Left	T2	N0	M0	IIA	Invasive carcinoma
11	82	F	II-III	Yes	Right	T2	N0	M0	IIA	Invasive carcinoma
12	63	F	II	Yes	Left	T2	N0	M0	IIA	Invasive carcinoma
13	53	F	II	Yes	Right	T2	N0	M0	IIA	Invasive carcinoma
14	59	F	II	Yes	Left	T2	N0	M0	IIA	Invasive carcinoma
15	48	F	II	Yes	Right	T2	N0	M0	IIA	Invasive carcinoma
16	70	F	II-III	Yes	Left	T2	N0	M0	IIA	Invasive carcinoma
17	58	F	II-III	Yes	Right	T2	N0	M0	IIA	Invasive carcinoma
18	58	F	II-III	Yes	Right	T2	N0	M0	IIA	Invasive carcinoma
19	75	F	I-II	Yes	Right	T2	N0	M0	IIA	Invasive carcinoma
20	80	F	II	Yes	Left	T2	N0	M0	IIA	Invasive carcinoma
21	53	F	II-III	Yes	Left	T2	N0	M0	IIA	Invasive carcinoma
22	41	F	II-III	Yes	Left	T2	N1	M0	IIB	Invasive carcinoma
23	46	F	II	Yes	Left	T2	N1	M0	IIB	Invasive carcinoma
24	56	F	II-III	Yes	Right	T2	N1	M0	IIB	Invasive carcinoma
25	72	F	II	Yes	Right	T2	N1	M0	IIB	Invasive carcinoma
26	58	F	II-III	Yes	Right	T2	N1	M0	IIB	Invasive carcinoma
27	56	F	II-III	Yes	Right	T2	N1	M0	IIB	Invasive carcinoma
28	55	F	II	Yes	Right	T2	N1	M0	IIB	Invasive carcinoma
29	57	F	II	Yes	Right	T2	N1	M0	IIB	Invasive carcinoma
30	83	F	II	Yes	Left	T2	N1	M0	IIB	Invasive carcinoma
31	56	F	II	Yes	Right	T2	N2	M0	IIIA	Invasive carcinoma
32	38	F	II	Yes	Left	T2	N2	M0	IIIA	Invasive carcinoma
33	48	F	II	Yes	Left	T2	N2	M0	IIIA	Invasive carcinoma
34	43	F	II	Yes	Left	T2	N2	M0	IIIA	Invasive carcinoma
35	44	F	II	Yes	Right	T2	N2	M0	IIIA	Invasive carcinoma
36	47	F	II-III	Yes	Left	T2	N2	M0	IIIA	Invasive carcinoma
37	46	F	II	Yes	Left	T3	N1	M0	IIIA	Invasive carcinoma
38	56	F	II	Yes	Left	T1	N3	M0	IIIC	Invasive carcinoma
39	60	F	II-III	Yes	Left	T2	N3	M0	IIIC	Invasive carcinoma
40	37	F	I-II	Yes	Left	T2	N3	M0	IIIC	Invasive carcinoma
41	58	F	III	Yes	Right	T2	N3	M0	IIIC	Invasive carcinoma
42	64	F	II-III	Yes	Right	T2	N3	M0	IIIC	Invasive carcinoma
43	42	F	II-III	Yes	Left	T3	N3	M0	IIIC	Invasive carcinoma
44	42	F	II	Yes	Right	T3	N3	M0	IIIC	Invasive carcinoma
45	40	F	II	Yes	Right	T3	N3	M0	IIIC	Invasive carcinoma

Neoplasm Disease Stage was determined according to NCCN guidelines of breast cancer.

Table S2. The demographic and clinicopathological features of another cohort of 8 breast cancer patients

Patient	Age	Gender	Histological type	Other malignancy history	Laterality	Tumor size	Lymph node invasion stage	Distant metastasis	TNM Stage	Other disease history
1	50	F	HER2+	No	Left	T2	N1	No	IIB	No
2	51	F	Luminal B	No	Left	T2	N0	No	IIA	No
3	55	F	Luminal B	No	Right	T1	N0	No	IA	No
4	74	F	HER2+	No	Right	T2	N0	No	IIA	Hypertension, Diabetes
5	51	F	Luminal B	No	Left	T2	N0	No	IIA	No
6	52	F	Luminal B	No	Left	T2	N1	No	IIB	No
7	48	F	Luminal B	No	Left	T2	N0	No	IA	No
8	54	F	HER2+	No	Left	T1	N0	No	IB	Hypertension

Neoplasm Disease Stage was determined according to NCCN guidelines of breast cancer.

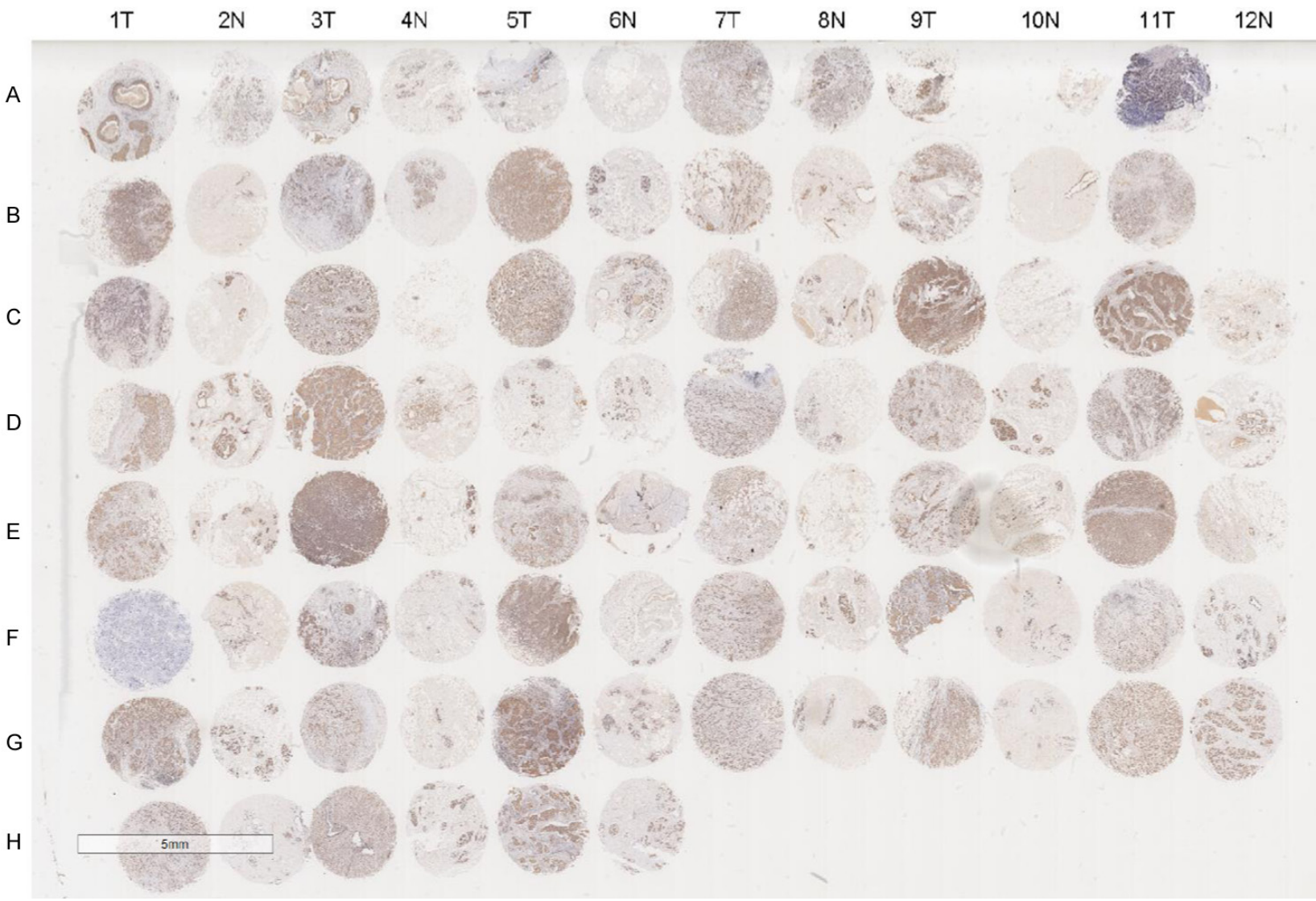

Figure S1. PSMD7 expression is upregulated in tumor tissues from breast cancer patients. Specificity and cellular localization of PSMD7 were demonstrated in patients' breast invasive ductal carcinoma (IDC) tissues. A total of 45 paired non-cancerous and tumor tissues from IDC patients were stained with anti-PSMD7 antibody. Scale bar, 5 mm. N, non-tumorous control tissues; T, IDC tumor tissues.

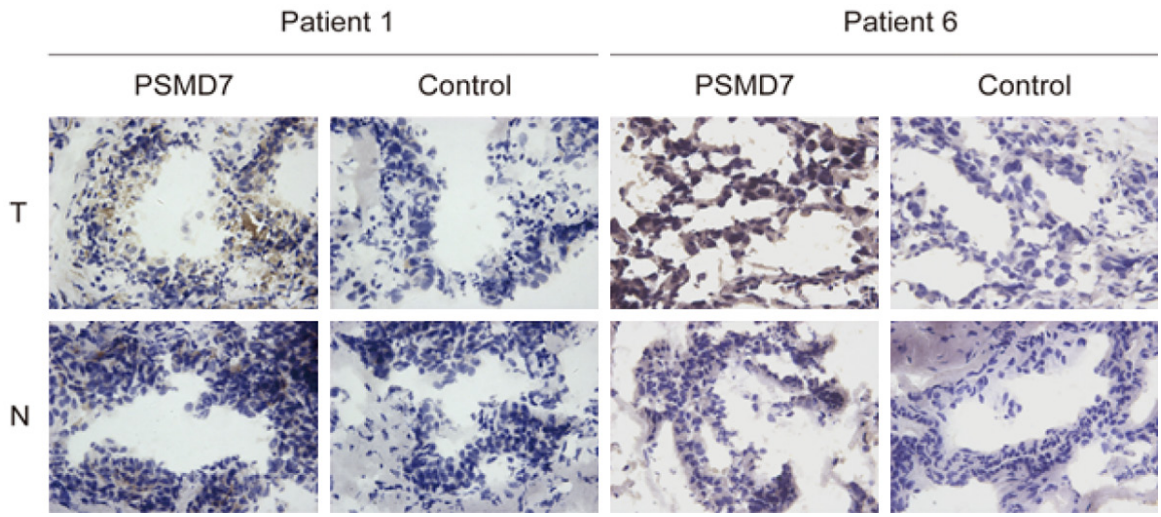

Figure S2. PSMD7 expression is upregulated in iced tumor tissues from breast cancer patients. The typical IHC staining of PSMD7 in the tumor and paired adjacent non-cancerous iced tissues from breast cancer patients is shown. Isotype normal IgG was used as a control antibody to stain tumor and non-tumorous tissues. Magnification: 400 ×.